Copper(II) Compounds Extended by 5-Carboxysalicylaldehyde and Its Schiff Bases: Interplay of Two Metal-Binding Sites and Intermolecular Stacking Contributing to Their Network and Bulk Structures

Reki Sakamoto, Masaaki Ohba, Nobuo Fukita, Kazuhiro Takahashi, Hisashi Ōkawa,* and Laurence K. Thompson†

Department of Chemistry, Faculty of Science, Kyushu University, Hakozaki 6-10-1, Higashi-ku, Fukuoka 812-8581

†Department of Chemistry, Memorial University of Newfoundland, St. John's, Newfoundland A1B 3X7, Canada

(Received June 8, 1998)

5-Carboxysalicylaldehyde (H_2casal) formed two mixed-ligand complexes, [Cu(Hcasal)(bpy)]ClO_4 (**1**) and [Cu(casal)(bpy)]·$2H_2O$ (**2**) (bpy = 2,2′-bipyridine) and the Schiff bases H_2L^1 and H_2L^2 derived by condensing H_2casal with *N*,*N*-dimethylethylenediamine and bis(3-aminopropyl)amine, respectively, formed [Cu(L^1)]·$0.25H_2O$ (**3**) and [Cu(L^2)]·H_2O (**4**), respectively. X-Ray crystallographic studies were done for **1**, [Cu(casal)(bpy)(MeOH)] (**2′**), [Cu(L^1)]·$4H_2O$ (**3′**) and **4**. **1**: Monoclinic, space group *C*2/*c*, a = 18.457(5), b = 19.215(5), c = 12.237(3) Å, α = 90, β = 121.76(2), γ = 90°, V = 3690(1) Å^3, and Z = 8. It has a dimeric structure with a perchlorato bridge between two [Cu(Hcasal)(bpy)]$^+$ moieties. In the bulk the dimeric units are assembled by interligand noncovalent interactions providing a pseudo 2-D sheet. **2′**: Monoclinic, space group $P2_1/m$, a = 9.791(4), b = 6.850(4), c = 25.56(1) Å, α = 90, β = 98.99(3), γ = 90°, V = 1692(1) Å^3, and Z = 4. The casal^{2-} combines one copper at the mixed-ligand site and the carboxylato group unidentately coordinates to the adjacent molecule, providing a 1-D zipper-like chain. The 1-D chains are further assembled through the interchain bpy/bpy stacking to form a pseudo 2-D network extended on the *bc* plane. **3′**: Tetragonal, space group $I4_1/a$, $a = b$ = 16.006(3), c = 27.745(7) Å, $\alpha = \beta = \gamma$ = 90°, V = 7108(2) Å^3, and Z = 16. It has a 1-D helical structure extended by Cu–NNO(spacer)OO–Cu linkages along *c* axis (Fig. 6): The nearest Cu–Cu separation in the chain is 9.60 Å. The four water molecules exist in the helical column but are readily removed in the air. **4**: Monoclinic, space group $P2_1/c$, a = 9.149(6), b = 17.566(6), c = 11.004(6) Å, α = 90, β = 110.03(4), γ = 90°, V = 1661(1) Å^3, and Z = 4. It has a 1-D zigzag chain structure extended by Cu–NNNO(spacer)O–Cu linkages. Further, the 1-D chains align through noncovalent interchain interaction to provide a pseudo 2-D sheet. The interplay of the two dissimilar metal-binding sites of H_2casal and its Schiff bases and the intermolecular noncovalent interaction contributing to the network and bulk structures of the complexes are discussed.

Crystal engineering of metal-extended systems is a current area of major research interest focusing on the production of advanced materials. The use of an appropriate bridging ligand is essential for constructing extended systems of metal ions. A typical example is the oxalate ion which produces 1-D,[1] 2-D,[2—4] and 3-D[5] metal-extended systems with a rather short metal–metal separation (5.1—5.2 Å). The heterobimetallic systems extended by oxalate bridges form a family of ferro- and ferrimagnets exhibiting spontaneous magnetization.[6—11] Bridging ligands having two metal-binding sites separated by a 'spacer' give a larger separation between the nearest metal centers. Terephthalic acid and fumaric acid are examples of such 'spacer'-based bridging ligands. Mori et al.[12] employed these dicarboxylic acids to provide 2-D Cu^{II}- and Mo^{II}-extended systems that act as hosts for inclusion of guest molecules.

Unsymmetric bridging ligands having two dissimilar metal-binding sites are of particular interest in the interplay of the two sites in constructing a specific network of a metal-extended system. In order to illustrate such an interplay of two dissimilar metal-binding sites in a network formation, 5-carboxysalicylaldehyde (H_2casal) is adopted in this work: It has the bidentate 'salicylaldehyde' site and the mono- or didentate 'carboxyl' site, separated by the aromatic entity (Scheme 1). Further, Schiff-bases were derived by condensing H_2casal with *N*,*N*-dimethylethylenediamine (abbreviated as H_2L^1) or with bis(3-aminopropyl)amine (H_2L^2) (see Scheme 1). The former has a tridentate metal-binding site of the NNO donor set and the latter has a tetradentate site of the NNNO donor set, instead of the didentate 'salicylaldehyde' site of the OO set of H_2casal. Mixed-ligand copper(II) complexes of H_2casal, [Cu(Hcasal)(bpy)]ClO_4 (**1**) and [Cu(casal)(bpy)]·$2H_2O$ (**2**) (bpy = 2,2′-bipyridyl), and copper(II) complexes of the Schiff bases, [Cu(L^1)]·$0.25H_2O$ (**3**) and [Cu(L^2)]·H_2O (**4**), have been obtained and their crystal and network structures are determined. Emphasis is placed on the interplay of the two dissimilar metal-binding sites of the bridging ligands and the intermolecular

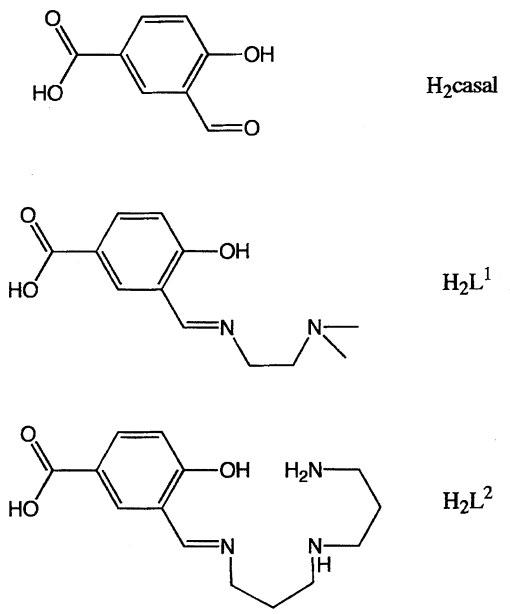

Scheme 1. Chemical structures of H_2casal, H_2L^1, and H_2L^2.

stacking contributing to the network structures of the complexes.

Experimental

Measurements. Elemental analyses of carbon, hydrogen and nitrogen were obtained at the Service Center of Elemental Analysis of Kyushu University. Copper analyses were made on a Shimadzu AA-680 Atomic absorption/Flame Emission on Spectrophotometer. Infrared spectra were measured using KBr disks on a JASCO IR-810 spectrophotometer. Electronic spectra were recorded on a Shimadzu MPS-2000 spectrometer. ESR spectra were recorded on a JEOL JEX-FE3X spectrometer. Magnetic susceptibilities were measured on a Faraday balance in the temperature range of 80—300 K and on a Quantum Design MPMS2 SQUID susceptometer in the range of 4.3—80 K.

Materials. Unless otherwise stated, all chemicals were purchased from commercial sources and used without further purification. Solvents were purified and dried by standard methods. 5-Carboxysalicylaldehyde (H_2casal) was prepared by the literature method.[13—15]

Preparation. [Cu(Hcasal)(bpy)]ClO_4 (1). Copper(II) perchlorate hexahydrate (185 mg, 0.5 mmol) and 2,2′-bipyridine (bpy) (78 mg, 0.5 mmol) were dissolved in an aqueous methanol (1 : 1 in volume, 30 cm^3). To this was added H_2casal (83 mg, 0.5 mmol) and the resulting green solution was allowed to stand for several days to give green crystals. They were collected by suction filtration, washed with a small amount of methanol and dried in vacuo. The yield was 160 mg (66%). Anal. Calcd for $C_{18}H_{13}O_8N_2ClCu$: C, 44.64; H, 2.71; N, 5.78; Cu, 13.12%. Found: C, 44.83; H, 2.65; N, 5.75; Cu, 12.02%. μ_{eff} per Cu: 1.81 μ_B at 290 K. Selected IR [ν/cm^{-1}] using KBr 3125, 3060, 1722, 1620, 1535, 1458, 1405, 1178, 1135, 1100, 1063, 773, 690, 622 cm^{-1}. UV-vis [λ_{max}/nm (ε/M^{-1} cm^{-1})]: 620 (107) in methanol; 595 on powdered sample (1 M = 1 mol dm^{-3}).

[Cu(casal)(bpy)]·2H_2O (2). This was prepared as green needles in a way similar to that of **1**, except for the use of copper(II) acetate monohydrate instead of copper(II) perchlorate hexahydrate. The crystals showed an efflorescent nature in the open air. The yield was 180 mg (86%). Anal. Calcd for $C_{18}H_{16}O_6N_2Cu$: C, 51.49; H, 3.84; N, 6.67; Cu, 15.13%. Found: C, 51.54; H, 3.74; N, 6.60; Cu, 14.37%. μ_{eff} per Cu: 1.82 μ_B at 290 K. Selected IR [ν/cm^{-1}] using KBr 3075, 1622, 1562, 1400, 1350, 1180, 1122, 795, 780, 708 cm^{-1}. UV-vis [λ_{max}/nm] on powdered sample: 650.

Single crystals of [Cu(casal)(bpy)(MeOH)] (**2′**) suitable for X-ray crystallography were grown from a DMF-methanol solution of **2**.

[Cu(L^1)]·0.25H_2O (3). To a stirred suspension of [Cu(Hcasal)$_2$]·H_2O (103 mg, 0.25 mmol) in methanol (30 cm^3) were added DBU (1,8-diazabicyclo[5.4.0]undec-7-ene; 76 mg, 0.5 mmol), copper(II) perchlorate hexahydrate (93 mg, 0.25 mmol) and *N*,*N*-dimethylethylenediamine (44 mg, 0.5 mmol) at room temperature. The resulting green solution was filtered once to separate any insoluble material, diluted with water (10 cm^3) and allowed to stand for several days to give dark blue crystals of the tetrahydrate [Cu(L^1)]·4H_2O (**3′**). The crystals effloresced in air to give almost anhydrous **3**. The yield was 70 mg (46%). Anal. Calcd for $C_{12}H_{14.5}O_{3.25}N_2Cu$: C, 47.68; H, 4.84; N, 9.27%. Found: C, 47.99; H, 4.66; N, 9.17%. μ_{eff} per Cu: 1.86 μ_B at 300 K. Selected IR [ν/cm^{-1}] using KBr 2890, 2865, 2818, 1640, 1607, 1370, 1322, 1192, 788, 695, 650 cm^{-1}. UV-vis [λ_{max}/nm] on powdered sample: 655.

[Cu(L^2)]·H_2O (4). This was prepared as green crystals in a way similar to that of **3** using bis(3-aminopropyl)amine. The yield was 60 mg (35%). Anal. Calcd for $C_{14}H_{21}O_4N_3Cu$: C, 46.85; H, 5.90; N, 11.71; Cu, 17.71% Found: C, 46.94; H, 5.89; N, 11.64; Cu, 17.58%. μ_{eff} per Cu: 1.85 μ_B at 300 K. Selected IR [ν/cm^{-1}] using KBr 3315, 3205, 2915, 2900, 2875, 1627, 1600, 1570, 1375, 1050, 795, 687 cm^{-1}. UV-vis [λ_{max}/nm] on powdered sample: 655.

X-Ray Structural Analyses. A single crystal of **1** was mounted on a glass fiber and coated with epoxy resin. Each crystal of **2′**, **3′**, and **4** was sealed in glass tubes. Intensities and lattice parameters were obtained on a Rigaku AFC-7R automated four-circle diffractometer with graphite-monochromated Mo $K\alpha$ radiation (λ = 0.71069 Å) and a 12 kW rotating anode generator. The data were collected at 20±1°C using the ω–2θ scan technique to a maximum 2θ value of 50.0° at a scan speed of 16.0° min^{-1} (in omega). The weak reflections ($I < 10.0\sigma(I)$) were rescanned (maximum of 4 scans) and the counts were accumulated to ensure good counting statistics. Stationary background counts were recorded on each side of the reflection. The ratio of peak counting time to background counting time was 2 : 1. The diameter of the incident beam collimator was 1.0 mm, the crystal to detector distance was 235 mm, and the computer controlled detector aperture was set to 9.0×13.0 mm (horizontal×vertical). The cell parameters were determined by 25 reflections in the 2θ range of 22.37° < 2θ < 24.94° for **1**, 6.47° < 2θ < 14.24° for **2′**, 28.80° < 2θ < 29.74° for **3′** and 29.39° < 2θ < 30.01° for **4**. The octant measured was +h, −k, ±l for **1**, ±h, +k, −l for **2′**, +h, +k, +l for **3′** and +h, +k, ±l for **4**. Three standard reflections were monitored every 150 reflections. Over the course of data collection, the standards increased by 0.4% for **1**, decreased by 4.9% for **2′**, decreased by 0.3% for **3′** and increased by 0.1% for **4**. A linear correction factor was applied to the data to account for the phenomena. The linear absorption coefficient, μ, for Mo $K\alpha$ radiation was 13.8 cm^{-1} for **1**, 13.3 cm^{-1} for **2′**, 12.6 cm^{-1} for **3′** and 13.3 cm^{-1} for **4**. An empirical absorption correction based on azimuthal scans of several reflections was applied. This resulted in transmission factors ranging from 0.80 to 1.00 for **1**, from 0.83 to 1.00 for **2′**, from 0.82 to 1.00 for **3′** and from 0.91 to 1.00 for **4**. Intensity data were corrected for Lorentz and polarization effects. Crystal data parameters for **1**, **2′**, **3′**, and **4** are given in Table 1.

The structures were solved by direct methods and expanded using Fourier techniques. Non-hydrogen atoms were refined anisotropically. Hydrogen atoms were included in structure factor calculations. The final cycle of full-matrix least squares refinement of **1**, **2′**, **3′**, and **4** was based on 2580, 1716, 1434, and 1640 observed reflections ($I > 3.00\sigma(I)$), respectively, and 286, 290, 209, and 199 variable parameters, respectively. Unweighted and weighted agreement factors of the forms $R = \Sigma||F_o| - |F_c||/\Sigma|F_o|$ and $R_w = [(\Sigma w(|F_o| - |F_c|)^2/\Sigma wF_o^2]^{1/2}$ are used. The agreement factors R (R_w) of **1**, **2′**, **3′**, and **4** were 0.045 (0.032), 0.041 (0.036), 0.062 (0.073), and 0.075 (0.055), respectively. The final positional parameters of non-hydrogen atoms with their estimated standard deviations are listed in Tables 2, 3, 4, and 5.

Neutral atom scattering factors were taken from Cromer and Waber.[16] Anomalous dispersion effects were included in Fcalc; the values for Δf and $\Delta f'$ were those of Creagh and McAuley.[17] The values for the mass attenuation coefficients are those of Creagh and Hubbel.[18] All calculations were performed using the teXsan[19] crystallographic software package of Molecular Structure Corporation. The final atomic coordinates, thermal parameters, full bond distances and angles are deposited at the Cambridge Crystallographic Data Center.

Results and Discussion

Synthesis and General Characterization. In preliminary studies, H_2casal itself formed a bis-type copper(II) complex, $[Cu(Hcasal)_2]\cdot H_2O$, in which the carboxylato group in the protonated form is free from bridging to the neighboring copper center. To achieve the involvement of the carboxylate group in a copper-extended network, a modulation of the 'salicylaldehyde' site is needed so as to reserve positive charge at the bound copper center and to provide a coordinative unsaturation about the copper (three- or four-coordination) for the carboxylato coordination. One promising approach in this line can be a mixed-ligand chromophore $\{Cu(OO)(NN)\}^+$ with a bidentate diamine ligand. Thus, a copper(II) salt, H_2casal and 2,2′-bipyridine (bpy) were reacted in the 1 : 1 : 1 molar ratio. The reaction using copper(II) perchlorate hexahydrate as the metal salt gave [Cu(Hcasal)(bpy)]ClO_4 (**1**) having a protonated carboxy group, whereas the reaction using copper(II) acetate monohydrate gave [Cu(casal)(bpy)]$\cdot 2H_2O$ (**2**) having a deprotonated carboxylato group. In another approach, H_2casal was converted into

Table 2. Atomic Coordinates and Equivalent Isotropic Thermal Parameters of Non-Hydrogen Atoms for [Cu(Hcasal)(bpy)]ClO_4 (**1**)

Atom	x	y	z	B(eq)
Cu(1)	0.13965(3)	0.19345(3)	0.13959(5)	3.13(1)
Cl(1)	0	0.12750(9)	1/4	3.19(4)
Cl(2)	1/2	0.0526(1)	1/4	5.22(5)
O(1)	0.0485(2)	0.2311(2)	−0.0124(3)	3.89(7)
O(2)	0.1156(2)	0.0987(2)	0.0743(3)	3.45(7)
O(3)	−0.2778(2)	0.1388(2)	−0.5241(3)	5.13(9)
O(4)	−0.2336(2)	0.0331(2)	−0.4422(3)	5.3(1)
O(5)	0.0636(2)	0.1713(2)	0.2536(4)	6.9(1)
O(6)	−0.0361(2)	0.0872(2)	0.1379(3)	7.2(1)
O(7)	1/2	−0.0181(3)	1/4	9.1(2)
O(8)	0.486(1)	0.0632(7)	0.122(1)	11.5(5)
O(9)	0.4409(7)	0.0898(7)	0.162(2)	12.9(5)
O(10)	0.4175(5)	0.0739(5)	0.234(1)	6.1(3)
N(1)	0.2462(2)	0.1678(2)	0.3016(3)	3.23(9)
N(2)	0.1751(2)	0.2877(2)	0.2142(3)	3.04(9)
C(1)	−0.0129(3)	0.1970(2)	−0.1101(4)	3.0(1)
C(2)	−0.0167(3)	0.1236(2)	−0.1187(4)	2.8(1)
C(3)	−0.0874(3)	0.0912(2)	−0.2273(4)	3.1(1)
C(4)	−0.1505(3)	0.1303(2)	−0.3240(4)	2.9(1)
C(5)	−0.1439(3)	0.2033(3)	−0.3160(4)	3.3(1)
C(6)	−0.0771(3)	0.2361(2)	−0.2138(4)	3.4(1)
C(7)	0.0496(3)	0.0800(2)	−0.0266(4)	3.3(1)
C(8)	−0.2235(3)	0.0945(3)	−0.4343(4)	3.7(1)
C(9)	0.2870(3)	0.2211(2)	0.3809(4)	3.0(1)
C(10)	0.3625(3)	0.2112(3)	0.4978(4)	4.1(1)
C(11)	0.3942(3)	0.1449(3)	0.5323(5)	4.9(1)
C(12)	0.3526(3)	0.0907(3)	0.4530(5)	4.9(1)
C(13)	0.2783(3)	0.1029(3)	0.3374(5)	4.3(1)
C(14)	0.2463(3)	0.2894(2)	0.3328(4)	3.0(1)
C(15)	0.2769(3)	0.3521(3)	0.3996(4)	4.0(1)
C(16)	0.2322(4)	0.4120(3)	0.3429(5)	5.0(2)
C(17)	0.1603(3)	0.4099(3)	0.2234(5)	4.7(1)
C(18)	0.1333(3)	0.3470(3)	0.1610(4)	3.8(1)

Table 1. Crystal Parameters for **1**, **2′**, **3′**, and **4**

Complex	**1**	**2′**	**3′**	**4**
Formura	$C_{18}H_{13}O_8N_2ClCu$	$C_{19}H_{16}O_5N_2Cu$	$C_{12}H_{22}O_7N_2Cu$	$C_{14}H_{21}O_4N_3Cu$
Formula weight	484.31	415.89	369.86	358.88
Crystal color	Dark blue	Green	Dark blue	Green
Crystal system	Monoclinic	Monoclinic	Tetragonal	Monoclinic
Space group	C_2/c (#15)	$P2_1/m$ (#14)	$I4_1/a$ (#88)	$P2_1/c$ (#14)
a/Å	18.457(5)	9.791(4)	16.006(3)	9.149(6)
b/Å	19.215(5)	6.850(4)	16.006(3)	17.566(6)
c/Å	12.237(3)	25.56(1)	27.745(7)	11.004(6)
β/°	121.76(2)	98.99(3)	90	110.03(4)
V/Å^3	3690(1)	1692(1)	7108(2)	1661(1)
Z value	8	4	16	4
D_{calc}/g cm^{-3}	1.743	1.632	1.382	1.435
μ(Mo $K\alpha$)/cm^{-1}	13.81	13.26	12.60	13.35
No. Observation	2580	1716	1434	1640
R	0.045	0.041	0.062	0.075
R_w	0.032	0.035	0.073	0.055

Table 3. Atomic Coordinates and Equivalent Isotropic Thermal Parameters of Non-Hydrogen Atoms for [Cu(casal)(bpy)(MeOH)] (**2′**)

Atom	*x*	*y*	*z*	*B*(eq)
Cu(1)	0.56574(7)	0.3516(1)	0.36480(3)	3.12(2)
O(1)	0.4886(3)	0.4165(6)	0.2934(1)	3.0(1)
O(2)	0.7485(4)	0.2926(6)	0.3471(1)	3.1(1)
O(3)	0.8370(4)	0.1971(6)	0.1108(1)	3.6(1)
O(4)	0.6254(4)	0.2373(8)	0.0647(1)	5.7(1)
O(5)	0.4932(5)	−0.0214(8)	0.3448(2)	6.6(2)
N(1)	0.3831(4)	0.3751(7)	0.3898(2)	2.6(1)
N(2)	0.6241(5)	0.2723(7)	0.4399(2)	2.5(1)
C(1)	0.5433(5)	0.3735(9)	0.2518(2)	2.3(1)
C(2)	0.6790(5)	0.2993(8)	0.2530(2)	2.1(1)
C(3)	0.7304(6)	0.2613(9)	0.2054(2)	2.3(1)
C(4)	0.6534(6)	0.2889(9)	0.1564(2)	2.7(1)
C(5)	0.5198(6)	0.363(1)	0.1557(2)	3.3(1)
C(6)	0.4663(5)	0.406(1)	0.2005(2)	3.2(1)
C(7)	0.7715(6)	0.270(1)	0.3014(2)	2.7(1)
C(8)	0.7079(7)	0.237(1)	0.1061(2)	3.3(2)
C(9)	0.3856(6)	0.3262(9)	0.4414(2)	2.5(1)
C(10)	0.2656(7)	0.327(1)	0.4639(2)	3.4(2)
C(11)	0.1431(7)	0.375(1)	0.4336(3)	4.2(2)
C(12)	0.1403(6)	0.422(1)	0.3812(3)	4.1(2)
C(13)	0.2616(6)	0.420(1)	0.3601(2)	3.4(2)
C(14)	0.5220(6)	0.2726(8)	0.4697(2)	2.4(1)
C(15)	0.5478(6)	0.2215(9)	0.5232(2)	2.8(1)
C(16)	0.6805(7)	0.171(1)	0.5449(2)	3.3(2)
C(17)	0.7838(6)	0.169(1)	0.5143(2)	3.5(2)
C(18)	0.7518(6)	0.221(1)	0.4616(2)	3.4(2)
C(19)	0.4216(8)	−0.066(1)	0.2961(4)	5.7(3)

Table 4. Atomic Coordinates and Equivalent Isotropic Thermal Parameters of Non-Hydrogen Atoms for [Cu(L′)]·4H_2O (**3′**)

Atom	*x*	*y*	*z*	*B*(eq)
Cu(1)	0.4674(1)	0.0779(1)	0.08816(5)	4.59(4)
O(1)	0.5813(5)	0.1084(5)	0.0751(3)	5.8(2)
O(2)	0.8046(5)	0.2521(5)	−0.0938(2)	5.2(2)
O(3)	0.6880(5)	0.2361(5)	−0.1328(3)	5.6(2)
O(4)	0.097(2)	0.477(2)	0.0101(7)	26(1)
O(5)	0.067(1)	0.082(1)	0.104(1)	24(1)
O(6)	0.4024(9)	0.078(1)	0.5870(5)	14.6(5)
O(7)	0.603(2)	0.164(2)	0.521(1)	20(1)
O(8)	0.914(2)	0.162(4)	0.064(1)	24(2)
N(1)	0.4324(6)	0.1004(5)	0.0223(3)	4.1(2)
N(2)	0.3422(6)	0.0628(6)	0.1000(3)	5.0(3)
C(1)	0.6141(8)	0.1361(7)	0.0353(4)	4.5(3)
C(2)	0.5656(7)	0.1481(6)	−0.0079(4)	3.8(3)
C(3)	0.6064(7)	0.1790(7)	−0.0488(3)	4.0(3)
C(4)	0.6891(7)	0.1981(7)	−0.0499(3)	3.8(3)
C(5)	0.7356(7)	0.1856(7)	−0.0083(4)	4.5(3)
C(6)	0.6987(7)	0.1555(8)	0.0333(4)	4.9(3)
C(7)	0.4778(7)	0.1282(6)	−0.0113(4)	3.7(3)
C(8)	0.7277(8)	0.2308(7)	−0.0955(4)	4.5(3)
C(9)	0.3434(7)	0.0870(8)	0.0131(4)	5.1(3)
C(10)	0.3088(8)	0.0341(8)	0.0517(5)	5.8(4)
C(11)	0.307(1)	0.141(1)	0.1134(6)	8.7(5)
C(12)	0.3169(9)	−0.001(1)	0.1352(5)	6.7(4)

Table 5. Atomic Coordinates and Equivalent Isotropic Thermal Parameters of Non-Hydrogen Atoms for [Cu(L^2)]·H_2O (**4**)

Atom	*x*	*y*	*z*	*B*(eq)
Cu(1)	0.1160(2)	0.72958(8)	0.1277(1)	3.36(3)
O(1)	0.179(1)	0.6343(4)	0.2184(7)	3.9(2)
O(2)	−0.050(1)	0.2957(4)	0.2241(7)	4.2(2)
O(3)	−0.259(1)	0.3419(5)	0.0740(9)	5.9(3)
O(4)	0.476(1)	0.092(1)	0.363(1)	17.8(6)
N(1)	−0.102(1)	0.6940(5)	0.0561(9)	3.0(2)
N(2)	0.086(1)	0.8172(6)	−0.0045(9)	3.6(3)
N(3)	0.349(1)	0.7511(6)	0.211(1)	5.1(3)
C(1)	0.109(1)	0.5680(7)	0.198(1)	3.3(3)
C(2)	−0.050(1)	0.5596(7)	0.119(1)	2.9(3)
C(3)	−0.117(1)	0.4875(7)	0.105(1)	3.1(3)
C(4)	−0.043(2)	0.4243(7)	0.166(1)	3.2(3)
C(5)	0.111(2)	0.4322(7)	0.240(1)	3.7(3)
C(6)	0.186(1)	0.5010(7)	0.257(1)	3.5(3)
C(7)	−0.142(1)	0.6247(7)	0.060(1)	3.1(3)
C(8)	−0.122(2)	0.3485(8)	0.152(1)	3.7(4)
C(9)	−0.225(1)	0.7496(7)	0.000(1)	4.1(3)
C(10)	−0.198(1)	0.7969(8)	−0.103(1)	5.1(4)
C(11)	−0.068(2)	0.8537(7)	−0.055(1)	4.4(4)
C(12)	0.202(2)	0.8786(7)	0.037(1)	5.9(4)
C(13)	0.376(2)	0.8512(9)	0.067(1)	6.4(5)
C(14)	0.443(2)	0.8153(8)	0.195(1)	6.3(4)

Schiff bases, H_2L^1 and H_2L^2, by condensing it with *N*,*N*-dimethylethylenediamine and bis(3-aminopropyl)amine, respectively. H_2L^1 has a uninegative tetradentate chelating site (NNO donor set) and H_2L^2 has a uninegative tetradentate chelating site (NNNO donor set). For practical purposes, the Schiff base complexes **3** and **4** were obtained by the reaction of [Cu(Hcasal)$_2$]·H_2O with *N*,*N*-dimethylethylenediamine and bis(3-aminopropyl)amine, respectively, under alkaline conditions in the presence of DBU.

Selected IR spectral data of **1**—**4** are given in the Experimental section. The complex **1** shows the ν(C=O) mode of the carboxylato group at 1720 cm^{-1}. This vibration is replaced by two carboxylato bands (ν_{as}(COO) and ν_s(COO)) at 1562 and 1350 cm^{-1} for **2**, 1565 and 1370 cm^{-1} for **3**, and 1570 and 1375 cm^{-1} for **4**. The difference between the two vibration modes for **2** and **4** is larger than 200 cm^{-1}, implying that there is the monodentate coordination of the carboxylato group in these compounds.[20] The mixed-ligand complexes **1** and **2** show the ν(C=O) mode of the formyl group near 1620 cm^{-1} together with the vibrations characteristic of bpy ligand. In the Schiff base complexes **3** and **4**, the aldehyde ν(C=O) mode is replaced by ν(C=N) mode of the azomethine group near 1630 cm^{-1}. The perchlorate ν_3 mode of **1** splits into three (1140, 1100, and 1060 cm^{-1}). This suggests a bidentate coordination of the perchlorate group.[21]

Visible spectra of **1**—**4** were measured by the reflectance technique on powdered samples or absorption in methanol solution. The numerical data are given in the Experimental section. When the reflectance spectra of **1** and **2** are compared, the former has a visible band maximum (superposition of d–d bands) at 595 nm, whereas the latter has a band max-

imum at 650 nm. The Schiff base complexes **3** and **4** coincidentally have d–d absorptions at the same wave-length (655 nm).

All the complexes have magnetic moments common for one unpaired electron. The magnetic moments of powdered samples showed little temperature-dependence down to liquid nitrogen temperature, suggesting that there is no appreciable magnetic interaction in the bulk. This is in accord with their ESR spectra (measured on powdered sample at liquid nitrogen temperature) which exhibit well-defined signals typical of an isolated spin located in an orbital of $d_{x^2-y^2}$ character.[22] Both **1** and **2** showed an axial ESR pattern; $g_{//} = 2.21$ and $g_{\perp} = 2.06$ for **1** and $g_{//} = 2.21$ and $g_{\perp} = 2.06$ for **2**. The ESR spectrum of **3′** is of an axial pattern with $g_{//} = 2.15$ and $g_{\perp} = 2.05$ whereas that of **4** is of a rhombic pattern with $g_1 = 2.17$, $g_2 = 2.13$, and $g_3 = 2.06$.

Crystal and Network Structures. [Cu(Hcasal)(bpy)]-ClO$_4$ (1). An ORTEP[23] view of the complex is shown in Fig. 1, together with the atom numbering scheme. The selected bond distances and angles with their estimated standard deviations are listed in Table 6.

The crystal consists of two $[Cu(Hcasal)(bpy)]^+$ cations and two perchlorate ions. One perchlorate ion is involved in the bridge between the two $[Cu(Hcasal)(bpy)]^+$ cations through its two oxygens, O(5) and O(5)*, forming a dimeric unit, whereas the other perchlorate is located in the crystal lattice. The Cu–Cu* separation in the dimeric unit is 6.97(1) Å. The geometry about each copper is square-pyramidal with O(1) and O(2) of the 'salicylaldehyde' site of Hcasal and N(1) and N(2) of the bpy on the equatorial base and O(5) of the bridging perchlorato ligand at the axial site. The basal bond distances fall in the range of 1.876(3)—1.985(3) Å. The axial Cu–O(5) bond distance (2.481(6) Å) is elongated owing to the Jahn–Teller effect of the d^9 electronic configuration. The $[Cu(Hcasal)(bpy)]^+$ part is almost planar. The deviation of Cu from the basal least-squares N_2O_2 plane toward the axial O(5) is small (0.069 Å). The two asymmetric $[Cu(Hcasal)(bpy)]^+$ cations in the dimeric unit are combined by

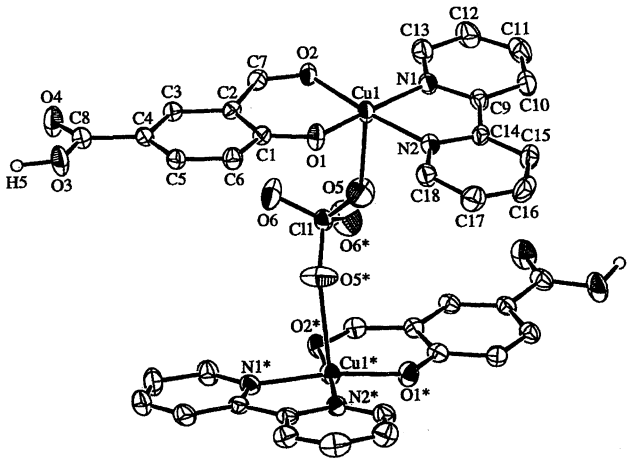

Fig. 1. An ORTEP view of the dinuclear core of [Cu(Hcasal)-(bpy)]ClO$_4$ (**1**) with the atom numbering scheme (non-coordinating perchlorate ion is omitted for clarity).

Table 6. Selected Bond Distances and Angles for **1**

	Bond distances (Å)		
Cu–O(1)	1.876(3)	Cu–O(2)	1.943(3)
Cu–O(5)	2.481(6)	Cu–N(1)	1.985(3)
Cu–N(2)	1.979(4)		
	Bond angles (deg)		
O(1)–Cu–O(2)	93.6(5)	O(1)–Cu–O(5)	98.4(1)
O(1)–Cu–N(1)	170.6(2)	O(1)–Cu–N(2)	90.6(1)
O(2)–Cu–O(5)	89.8(1)	O(2)–Cu–N(1)	94.0(1)
O(2)–Cu–N(2)	174.9(1)	O(5)–Cu–N(1)	87.3(2)
O(5)–Cu–N(2)	92.6(2)	N(1)–Cu–N(2)	81.6(1)
Cu–O(2)–C(7)	124.7(3)	Cu–O(1)–C(1)	127.2(3)
Cu–O(5)–Cl(1)	141.6(3)	Cu–N(1)–C(9)	114.7(3)
Cu–N(1)–C(13)	126.1(3)	Cu–N(2)–C(18)	126.1(2)

the symmetric operation $(-x, y, 1/2-z)$ through Cu–O(5)–Cl-(1)–O(5)*–Cu* bridge. The two $[Cu(Hcasal)(bpy)]^+$ planes in the unit are nearly parallel, with the average interatomic separation of ca. 7.09 Å, and are rotated by ca. 150° with respect to the Cu–Cu* axis.

In the bulk the dimeric units are assembled by the insertion of the bpy entity of one dimeric unit into the interspace of the adjacent dimeric unit, forming a pseudo 1-D chain running along the diagonal line of *a* and *c* axes (Fig. 2). The average bpy/bpy and bpy/casal separations are 3.63 and 3.76 Å, respectively, suggesting the operation of noncovalent interaction between the aromatic moieties. Further, the 1-D chains are assembled through the interchain casal/casal stacking to give a pseudo 2-D sheet: the average interatomic separation between the two casal entities is 3.48 Å.

[Cu(casal)(bpy)(MeOH)] (2′). An ORTEP diagram of the molecule is given in Fig. 3 together with the atom numbering scheme. Selected bond distances and angles are listed in Table 7.

The X-ray structure shows monodentate coordination of the casal carboxylato group to a copper center in an adjacent molecule to form a copper-extended compound. The copper atom assumes an axially-elongated six-coordinate environment with O(1) and O(2) of the 'salicylaldehyde' site and N(1) and N(2) of bpy on the basal plane and with the carboxylato O(3)* from the neighboring casal^{2-} ligand and the methanol oxygen O(5) at the axial sites. The basal Cu–N and Cu–O bond distances fall in the range of 1.914(3)—1.997(4) Å. The axial Cu–O(3)* and Cu–O(5) bond distances are 2.590 and 2.679(7) Å, respectively. The Cu(II) is displaced by 0.078 Å from the basal least-squares plane toward O(3).

In the bulk **2′** has a 1-D zipper-like structure running along the *b* axis (Fig. 4). In the chain, the casal ligands align in a stacked mode, but the separation between the adjacent casal planes is large (>4 Å). The one-dimensional chains are further assembled through the interchain bpy/bpy stacking to form a pseudo 2-D network extended on the bc plane. the average separation between the stacked bpy rings is 3.76 Å.

[Cu(L^1)]·4H$_2$O (3′). An ORTEP diagram of the molecule is given in Fig. 5, together with the atom num-

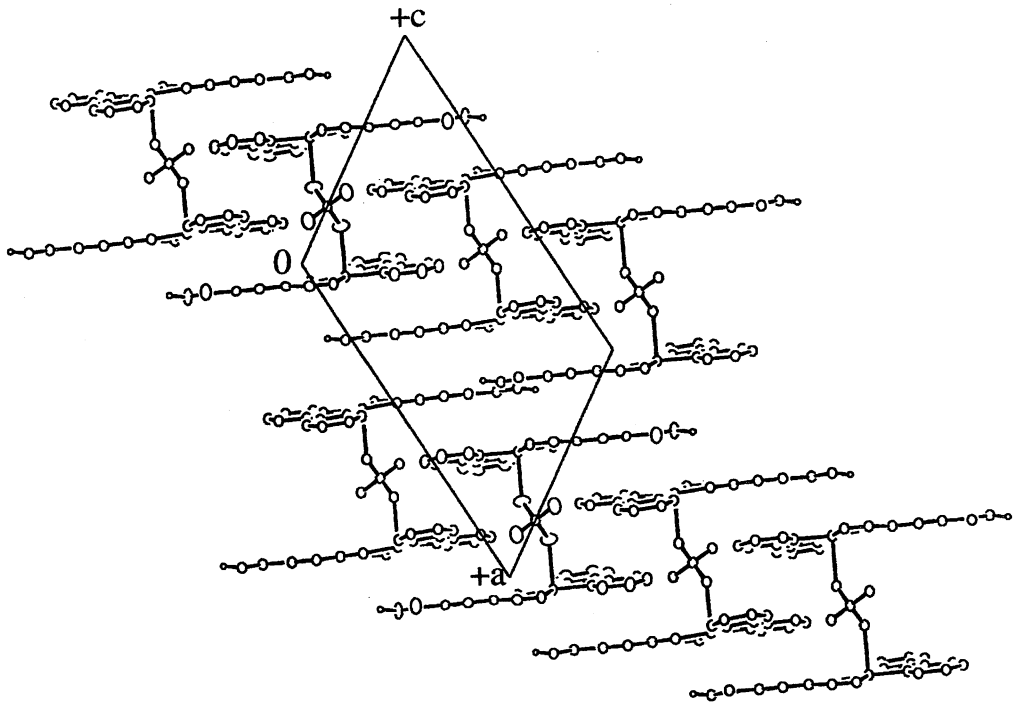

Fig. 2. A projection of the polymeric structure of **1** onto *bc* pane (non-coordinating perchlorate ions are omitted for clarity).

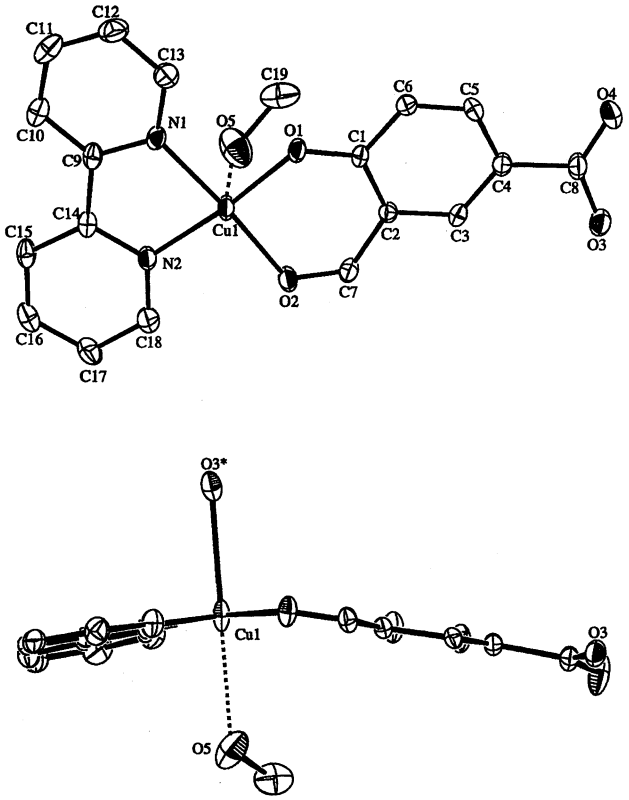

Fig. 3. An ORTEP view of [Cu(casal)(bpy)(MeOH)] (**2′**) with the atom numbering scheme.

Table 7. Selected Bond Distances and Angles for **2′**

	Bond distances (Å)		
Cu–O(1)	1.914(3)	Cu–O(2)	1.956(4)
Cu–O(3)	2.590(5)	Cu–N(1)	1.997(4)
Cu–N(2)	1.990(4)		
	Bond angles (deg)		
O(1)–Cu–O(2)	93.8(1)	O(1)–Cu–O(3)	95.3(2)
O(1)–Cu–N(1)	92.7(2)	O(1)–Cu–N(2)	173.3(2)
O(2)–Cu–O(3)	85.9(2)	O(2)–Cu–N(1)	171.2(2)
O(2)–Cu–N(2)	91.8(2)	O(3)–Cu–N(1)	99.4(2)
O(3)–Cu–N(2)	88.8(2)	N(1)–Cu–N(2)	81.4(2)
Cu–O(1)–C(1)	125.2(3)	Cu–O(2)–C(7)	123.7(4)
Cu–O(3)–C(8)	122.4(4)	Cu–N(1)–C(13)	126.5(4)
Cu–N(1)–C(9)	114.2(4)	Cu–N(2)–C(14)	114.7(4)
Cu–N(2)–C(18)	125.6(4)		

bering scheme. Selected bond distances and angles are listed in Table 8.

The crystal consists of one copper, one $(L^1)^{2-}$ in the fully-deprotonated form and four water molecules. The water molecules are not involved in coordination. The $(L^1)^{2-}$ combines one copper at the Schiff base site with its NNO donor set and another copper at the carboxylato group in the chelating mode, providing a five-coordinate environment about each copper. The geometry about the metal is depicted as a square-pyramid with N(1), N(2), and O(1) of the Schiff base site and O(2)* from the adjacent carboxylato group on the basal plane and O(3)* of the carboxylato group at an axial position. The in-plane bond distances fall in the range 1.922(8)—2.046(10) Å. The axial Cu–O(3)* bond distance is 2.494(8) Å. The deviation of Cu from the basal least-squares plane toward O(3)* is 0.0612 Å.

In the bulk **3′** forms a 1-D helical structure extended by the Cu–NNO(spacer)OO–Cu linkages along *c* axis (Fig. 6): the nearest Cu–Cu separation in the chain is 9.60 Å. No appreciable noncovalent interaction occurs between the chains. Figure 7 shows a projection of the network onto the *ab* plane,

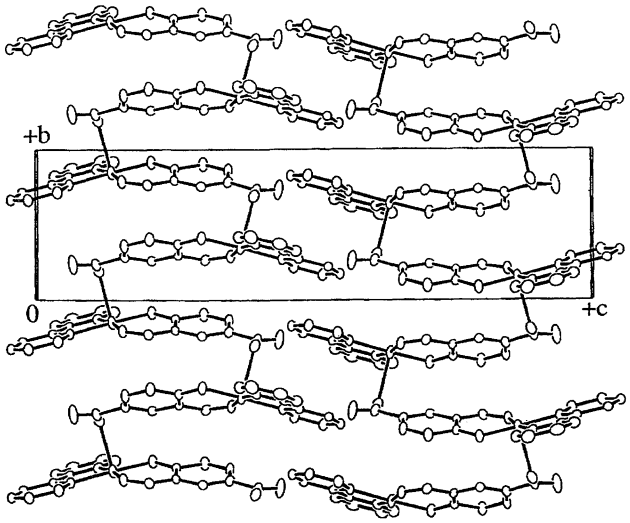

Fig. 4. A projection of **2′** onto *bc* pane (MeOH molecules are omitted for clarity).

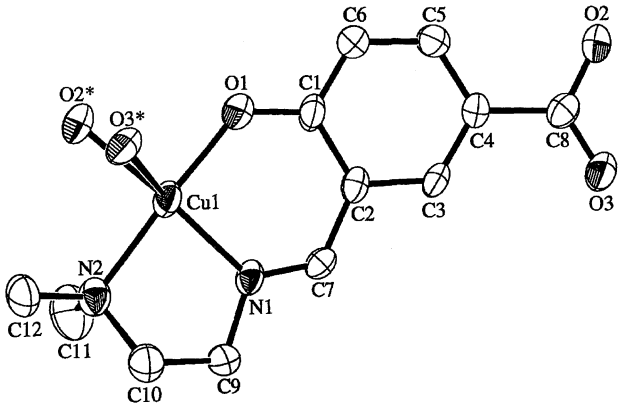

Fig. 5. An ORTEP view of $[Cu(L^1)]\cdot 4H_2O$ (**3′**) with the atom numbering scheme.

Table 8. Selected Bond Distances and Angles for **3′**

	Bond distances (Å)		
Cu–O(1)	1.922(8)	Cu–O(2)*	1.985(7)
Cu–O(3)*	2.494(8)	Cu–N(1)	1.944(8)
Cu–N(2)	2.046(10)		
	Bond angles (deg)		
O(1)–Cu–O(2)*	89.6(3)	O(1)–Cu–O(3)*	90.3(3)
O(1)–Cu–N(1)	92.8(4)	O(1)–Cu–N(2)	171.9(4)
O(2)*–Cu–O(3)	56.6(3)	O(2)*–Cu–N(1)	177.5(4)
O(2)*–Cu–N(2)	93.8(3)	O(3)*–Cu–N(1)	123.8(3)
O(3)*–Cu–N(2)	97.7(3)	N(1)–Cu–N(2)	83.7(4)
Cu–O(1)–C(1)	129.0(8)	Cu–O(2)*–C(8)	102.2(7)
Cu–O(3)*–C(8)	80.0(7)	Cu–N(1)–C(7)	126.4(8)
Cu–N(1)–C(9)	114.7(7)	Cu–N(2)–C(10)	103.9(7)
Cu–N(2)–C(12)	117.4(8)	Cu–N(2)–C(11)	109.2(9)

indicating that a square column is formed by the helical arrangement of the asymmetric units along a 4-fold axis (*c* axis). It is seen that both right-handed and left-handed helices exist in the lattice. The four water molecules are captured in the helical column but can be readily removed in the air.

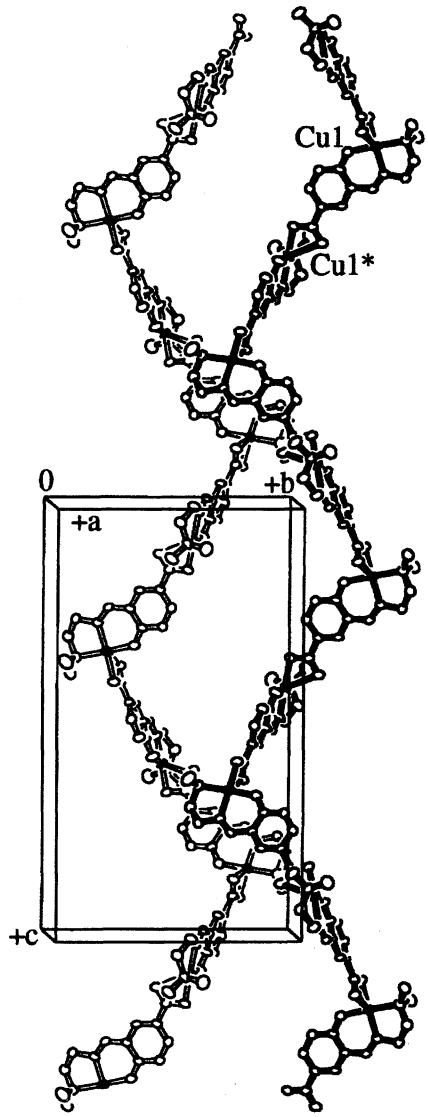

Fig. 6. A projection of **3′** onto *bc* pane indicating 1-D helical network (water molecules are omitted for clarity).

$[Cu(L^2)]\cdot H_2O$ (4). An ORTEP view of the complex is shown in Fig. 8 together with the atom numbering scheme. The selected bond distances and angles with their estimated standard deviations are listed in Table 9. A projection of the molecule onto the *bc* plane is shown in Fig. 9.

The X-ray structure reveals a one-dimensional zigzag chain structure extended by the Cu–NNNO(spacer)O–Cu linkages (see Fig. 9). Each copper has a nearly square-pyramidal geometry with N(1), N(2), N(3), and O(1) of the Schiff base site on the basal plane and O(2)* of the carboxylato site of the nearest molecule at the apical site. The in-plane bond distances fall in the range of 1.91(1)—2.07(1) Å. The axial Cu–O(2)* bond distance is 2.23 Å. The deviation of Cu from the basal least-squares plane toward O(2)* is 0.188 Å.

In the lattice, the 1-D zigzag chains align along the *b*-axis. The O(2)–C(8)–O(3) part of the carboxylato group is nearly coplanar with the aromatic ring and the Cu*–O(2) (Cu–O(2)*) bond is inclined by 94.8° to the basal least-squares

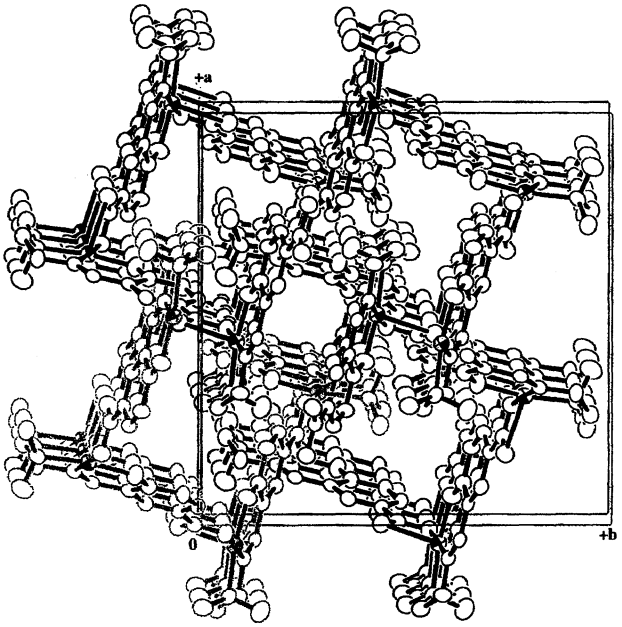

Fig. 7. A projection of **3′** onto *ab* pane (water molecules are omitted for clarity).

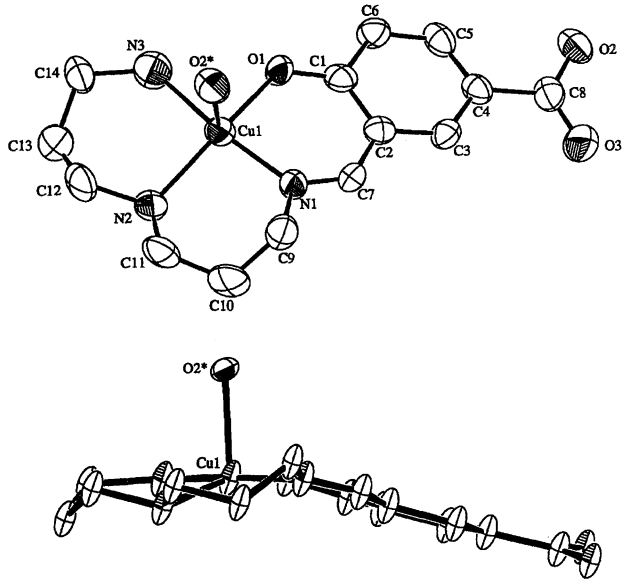

Fig. 8. An ORTEP view of $[Cu(L^2)]\cdot H_2O$ (**4**) with the atom numbering scheme.

plane. The Cu*–O(2) and Cu–O(2)* bonds are situated in a *cis* arrangement with respect to the mean molecular plane. There exists an interchain noncovalent interaction between casal entities. The average casal/casal separation is 3.6 Å (see Fig. 9).

From a detailed inspection of the crystal structures of **3′** and **4**, some geometrical differences can be pointed out. The average of the equatorial bond lengths is slightly shorter in **3′** (1.97 Å) relative to **4** (1.99 Å), whereas the axial Cu–O bond distance is longer in **3′** (2.49 Å) compared with **4** (2.23 Å). The displacement of Cu from the basal least-squares plane is small in **3′** (0.0612 Å) compared with **4** (0.188 Å). Further, the bite angles in the base range from 93.8° to 83.7° for **3′** and from 94.1° to 81.5° for **4**. Evidently, **4** shows a larger distortion in the basal plane from a regular square. This is reflected by a rhombic feature in the ESR spectrum of **4**.

Table 9. Selected Bond Distances and Angles for **4**

	Bond distances (Å)		
Cu–O(1)	1.91(1)	Cu–O(2)*	2.23(1)
Cu–N(1)	1.95(1)	Cu–N(2)	2.07(1)
Cu–N(3)	2.02(1)		
	Bond angles (deg)		
O(1)–Cu–O(2)*	99.1(5)	O(1)–Cu–N(1)	90.9(5)
O(1)–Cu–N(2)	162.5(5)	O(1)–Cu–N(3)	81.5(5)
O(2)*–Cu–N(1)	87.3(5)	O(2)*–Cu–N(2)	97.8(5)
O(2)*–Cu–N(3)	95.1(5)	N(1)–Cu–N(2)	94.1(5)
N(1)–Cu–N(3)	172.3(5)	N(2)–Cu–N(3)	92.8(5)
Cu–O(1)–C(1)	129(1)	Cu–O(2)–C(8)	128(1)
Cu–N(1)–C(7)	124(1)	Cu–N(1)–C(9)	118.8(9)
Cu–N(2)–C(12)	115(1)	Cu–N(2)–C(11)	118(1)
Cu–N(3)–C(14)	129(1)		

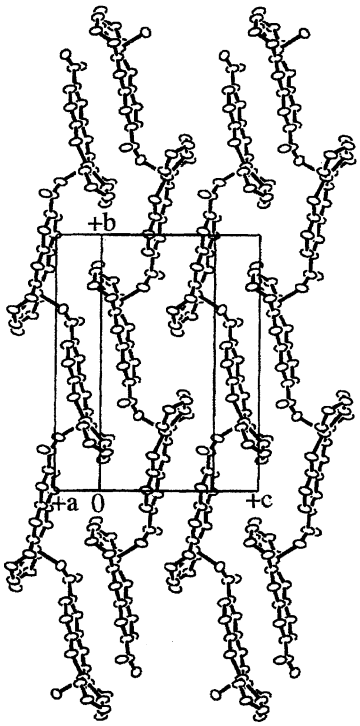

Fig. 9. A projection of **4** onto *bc* pane (water molecules are omitted for clarity).

Factors Contributing to Network and Bulk Structures. The variable coordination mode of the carboxylato site in **2′**, **3′**, and **4** can be explained in terms of the interplay with the other metal-binding site. In the case of **2′**, the carboxylato site acts as a monodentate ligand in conjunction with the tetradentate environment of the mixed-ligand chromophore {Cu(OO)(NN)}. This is also the case of **4**, where a tetradentate environment is provided by the Schiff base site of L^1. The resulting five-coordinate geometry about the metal in the associated structure of **2′** and **4** is common for Cu(II) with oxygen or nitrogen donor atoms. In the case of **3′**, the

carboxylato group acts as a bidentate chelating ligand in conjunction with the tridentate Schiff base site of L^2. That is, the bidentate or unidentate function of the carboxylato site is determined by the vacant site(s) for five-coordination at the copper center.

Another noticeable feature of **2′**, **3′**, and **4** is the stability of the networks in solution. The complex **2′** dissolves in methanol and **4** dissolves in water. This fact implies that the networks of **2′** and **4** collapse by solvation in a donor solvent. On the other hand, **3′** cannot be dissolved in most solvents, except for acidic solvents like acetic acid or aqueous mineral acid, indicating a significant stability of the helical network structure. This can be explained by the fact that the carboxylato group coordinates strongly to an equatorial site of copper(II) in **3′**, but weakly to an axial site of copper(II) in **2′** and **4**.

It must be mentioned that noncovalent interligand interactions can play an important role in the copper-extended networks of H_2casal and its Schiff bases. This effect is essential in the network structure of **1**; the perchlorate bridge between two $[Cu(Hcasal)(bpy)]^{2+}$ cations must have a secondary effect compared with the interligand stacking interaction observed (see Fig. 2). In the case of **2′** and **4**, the interligand interaction contributes the the 2-D ordering of the 1-D chains. On the other hand, the network structure of **3′** is controlled by the Cu–NNO(spacer)OO–Cu linkage. Evidently, the strong intermolecular coordination interaction is dominant in determining the network structure of **3′**, but the weak interligand noncovalent interaction plays an important role in determining the network structure when no intermolecular coordination interaction operates, as is the case of **1**, or this interaction is less effective, as is the case of **2′** and **4**.

This work was supported by a Grant-in-Aid for Scientific Research on Priority Area 'Metal-Assembled Complexes' (No. 10149106) and an International Scientific Research Program Grant (No. 09044093) from the Ministry of Education, Science, Sports and Culture.

References

1) J. J. Girerd, O. Kahn, and M. Verdaguer, *Inorg. Chem.*, **19**, 274 (1980).

2) L. O. Atovmyan, G. V. Shilov, R. N. Lyubovskaya, E. I. Zhilyaeva, N. S. Ovanesyan, S. I. Pirumova, I. G. Gusakovskaya, and Y. G. Morozov, *JETP Lett.*, **58**, 766 (1993).

3) S. Decurtins, H. W. Schmalle, H. R. Oswald, A. Linden, J. Ensling, P. Gutlich, and A. Hauser, *Inorg. Chim. Acta*, **216**, 65 (1994).

4) R. Pellaux, H. W. Schmalle, R. Huber, P. Fischer, T. Hauss, B. Ouladdiaf, and S. Decurtins, *Inorg. Chem.*, **36**, 2301 (1997).

5) S. Decurtins, H. W. Schmalle, P. Schneuwly, and H. R. Oswald, *Inorg. Chem.*, **32**, 1888 (1993).

6) Z. J. Zhong, N. Matsumoto, H. Ōkawa, and S. Kida, *Chem. Lett.*, **1990**, 87.

7) H. Tamaki, Z. J. Zhong, N. Matsumoto, S. Kida, M. Koikawa, N. Achiwa, Y. Hashimoto, and H. Ōkawa, *J. Am. Chem. Soc.*, **114**, 6974 (1992).

8) H. Ōkawa, N. Matsumoto, H. Tamaki, and M. Ohba, *Mol. Cryst. Liq. Cryst.*, **233**, 257 (1993).

9) H. Tamaki, M. Mitsumi, K. Nakamura, N. Matsumoto, S. Kida, H. Ōkawa, and S. Iijima, *Chem. Lett.*, **1992**, 1975.

10) H. Ōkawa, N. Matsumoto, H. Tamaki, and M. Ohba, *Mol. Cryst. Liq. Cryst.*, **233**, 257 (1993).

11) S. Iijima, T. Katsura, H. Tamaki, M. Mitsumi, N. Matsumoto, and H. Ōkawa, *Mol. Cryst. Liq. Cryst.*, **233**, 263 (1993).

12) W. Mori, F. Inoue, K. Yoshida, H. Nakayama, S. Takamizawa, and M. Kishita, *Chem. Lett.*, **1997**, 1219.

13) K. Reimer and F. Tiemann, *Ber.*, **9**, 1268 (1876).

14) D. E. Armstrong and D. H. Richardson, *J. Chem. Soc.*, **1933**, 496.

15) H. Wynberg, *Chem. Rev.*, **60**, 169 (1960).

16) D. T. Cromer and J. T. Waber, "International Tables for X-Ray Crystallography," Kynoch Press, Birmingham (1974), Vol. IV.

17) D. C. Creagh and W. J. Mcauley, "International Tables for Crystallography," ed by A. J. C. Wilson et al., Kluwer Acad. Pub., Boston (1992), pp. 219—222.

18) D. C. Creagh and J. H. Hubbell, "International Tables for Crystallography," ed by A. J. C. Wilson et al., Kluwer Acad. Pub., Boston (1992), pp. 200—206.

19) "TEXSAN," Molecular Structure Corporation, TX (1985).

20) G. B. Deason and R. J. Phillips, *Coord. Chem. Rev.*, **32**, 227 (1980).

21) K. Nakamoto, "Infrared Spectra of Inorganic and Coordination Compounds," 2nd ed, John Wiley & Sons, New York (1970), p. 175.

22) B. A. Goodman and J. B. Raynor, *Adv. Inorg. Chem. Radiochem.*, **13**, 135 (1970).

23) C. K. Johnson, "Report 3794," Oak Ridge National Laboratory, Oak Ridge, TN (1965).